Published in final edited form as:
Nature. 2009 July 9; 460(7252): 231–236. doi:10.1038/nature08159.

Mechanisms Promoting Translocations in Editing and Switching Peripheral B Cells

Jing H. Wang[1,2,3,4,7], **Monica Gostissa**[1,2,3,4,7], **Catherine T. Yan**[1,2,3,4,7], **Peter Goff**[1,2,3,4], **Thomas Hickernell**[1,2,3,4], **Erica Hansen**[1,2,3,4], **Simone Difilippantonio**[5], **Duane R. Wesemann**[1,2,3,4,6], **Ali A. Zarrin**[1,2,3,4,8], **Klaus Rajewsky**[3], **Andre Nussenzweig**[5], and **Frederick W. Alt**[1,2,3,4]

[1]Howard Hughes Medical Institute, Harvard Medical School

[2]The Children's Hospital, Harvard Medical School

[3]Immune Disease Institute, Harvard Medical School

[4]Department of Genetics, Harvard Medical School

[5]Experimental Immunology Branch, National Cancer Institute, National Institutes of Health

[6]Division of Rheumatology, Allergy and Immunology, Department of Medicine, Brigham and Women's Hospital

Abstract

V(D)J recombination assembles immunoglobulin (Ig) heavy or light chain (*IgH* or *IgL*) variable region exons in developing bone marrow B cells, while class switch recombination (CSR) exchanges *IgH* constant region exons in peripheral B cells. Both processes employ DNA double strand breaks (DSBs) repaired by non-homologous end-joining (NHEJ). Errors in either V(D)J recombination or CSR can initiate chromosomal translocations, including oncogenic *IgH/c-myc* translocations of peripheral B cell lymphomas. Collaboration between these processes also has been proposed to initiate translocations. However, occurrence of V(D)J recombination in peripheral B cells is controversial. Here, we report that activated NHEJ-deficient splenic B cells accumulate V(D)J recombination-associated *IgL* chromosomal breaks, as well as CSR-associated *IgH* breaks, often in the same cell. Moreover, *IgL* breaks frequently are joined to *IgH* breaks to form translocations, a phenomenon associated with specific *IgH/IgL* co-localization. *IgH* and *c-myc* also co-localize in these cells; correspondingly, introduction of frequent *c-myc* DSBs robustly promotes *IgH/c-myc* translocations. Our studies reveal peripheral B cells that attempt secondary V(D)J recombination and elucidate a role for mechanistic factors in promoting recurrent translocations in tumors.

[*]Correspondence and requests for materials should be addressed to Frederick W. Alt, Ph: 617-919-2539; Fax: 617-730-0948, alt@enders.tch.harvard.edu.
[7]These authors contributed equally to this work
[8]Current address: Ali A. Zarrin, Immunology Discovery Group, Genentech.

Supplementary Information is linked to the online version of the paper at www.nature.com/nature

Author contributions F.W.A., J.H.W., M.G. and C.T.Y. planned studies and interpreted data. J.H.W. performed the majority of experiments, including mouse breeding, B cell studies, FISH, and *IgH/Igλ* PCR studies. C.T.Y. bred mice and performed B cell analyses. M.G. generated and analyzed c-myc$^{25IsceI/wt}$ mice and performed FISH and I*gH/c-myc* translocation studies. P.G., T.H., and E.H. provided technical assistance. S.D. and A.N. provided expertise in 3D interphase FISH. A.A.Z. generated the 25 IsceI array. D.R.W. performed RAG expression studies and mesenteric lymph node B cell analyses. K.R. provided RAG conditional knock-out mice and helped interpret data. F.W.A., J.H.W. and M.G. wrote the paper.

Author information Reprints and permissions information is available at www.nature.com/reprints.

The authors declare no competing financial interests.

Recombination activating gene 1/2 (RAG) endonuclease initiates V(D)J recombination by cleaving V, D and J segments, which are joined exclusively by NHEJ to form V(D)J exons[1,2]. V(D)J recombination in bone marrow (BM) pro-B cells first assembles IgH V(D)J exons leading to μ chain expression[3]. Subsequently, IgL VJ exons are assembled in pre-B cells, generating immature B cells that express μ plus IgL chains as surface IgM[3]. The two IgL families (Igκ and Igλ) are encoded in distinct loci, and primary *Igκ* V(D)J recombination usually precedes that of *Igλ*[4]. Individual B cells express either Igκ or Igλ, with about 95% of mouse IgM^+ B cells being $Ig\kappa^+$ and the remainder $Ig\lambda^+$[4]. Newly generated BM B cells that express auto-reactive receptors can undergo tolerogenic secondary V(D)J recombination, termed receptor editing, in which they further rearrange or delete *Igκ* and may rearrange *Igλ*[5-7] (See Suppl. Fig. 1 for schematic version of these processes).

Surface IgM^+ B cells down-regulate RAG and migrate to peripheral lymphoid tissues (e.g. spleen) where they participate in antigen-dependent responses including CSR[8]. The various sets of germline *IgH* constant region exons ("C_H genes") are flanked by switch (S) regions[9]. Activation-induced cytidine deaminase (AID) initiates DSBs in Sμ and a downstream S region, which then are joined by NHEJ or, in its absence, by less efficient microhomology (MH)-mediated alternative end-joining (A-EJ)[9,10]. Thereby, Cμ is replaced with a downstream C_H gene to effect CSR (Suppl. Fig. 1). Germinal center (GC) B cells have been argued to undergo antigen-dependent secondary V(D)J recombination, termed "receptor revision", as a means of diversification[11]. Like receptor editing, receptor revision is proposed to target *Igκ* and *Igλ*, but to be distinct in location and activation mechanism[11,12]. However, whether or not V(D)J recombination occurs in the context of receptor revision in GC B cells has been debated[11-14].

Human and mouse B lymphomas often harbor clonal translocations linking oncogenes, such as *c-myc*, to *IgH*, *Igκ* or *Igλ*[15,16]. Such recurrent oncogenic translocations are thought to represent highly selected, very low frequency events. Even so, aspects of *c-myc*, beyond coding sequences, may increase its translocation fequency[17]. In this regard, loci involved in recurrent oncogenic translocations often are spatially proximal within interphase nuclei[18-23]. RAG and AID have been implicated in collaboratively initiating oncogenic translocations in human BM-derived pro-B/pre-B lymphomas[24,25]. Many oncogenic translocations in mature B lymphomas occur during attempted CSR and involve AID-initiated breaks[26-29]; but others result from RAG-initiated DSBs[15,30,31]. Due to checkpoint defects, RAG-initiated *IgH* breaks in ATM-deficient BM pro-B cells persist and can be translocation substrates in IgM^+ peripheral B cells[32]. Thus far, however, translocations have not been shown to result from RAG activity in peripheral B cells.

Xrcc4 is a critical NHEJ component[2]. In its absence, V(D)J recombination is abrogated[33,34] and CSR impaired[10,35]. Conditional inactivation of LoxP-flanked Xrcc4 in p53-deficient peripheral B cells via a CD21-Cre transgene leads to recurrent "CXP" B cell lymphomas that harbor aberrant *Igκ* and *Igλ* V(D)J rearrangements, *IgH* CSR events, and *Igλ* and/or *IgH/c-myc* translocations[36]. We proposed CXP tumor progenitors to be peripheral B cells that undergo secondary V(D)J recombination and CSR[36]. To search for such putative CXP tumor progenitors, we now have analyzed splenic "$CX^{c/-}$" B cells in which Xrcc4 was peripherally inactivated but p53 was left intact to obviate B cell lymphomas.

IgH Chromosomal Breaks in Xrcc4-Deficient Splenic B Cells are AID-dependent

$CX^{c/-}$ mice have normal IgM^+ B cell numbers, as *Xrcc4* is intact for primary V(D)J recombination in developing BM B cells, with inactivation starting in transitional stage

peripheral B cells[10,37]. $CX^{c/-}$ splenic B cells activated for CSR have high levels of *IgH* breaks on chromosome 12 due to impaired NHEJ[10]. While Xrcc4 deficiency is not associated with known checkpoint defects[34], we firmly tested AID-dependency of $CX^{c/-}$ B cell *IgH* breaks by breeding the $CX^{c/-}$ genotype onto an AID-deficient ($A^{-/-}$) background[38] to generate $CX^{c/-}A^{-/-}$ mice. We stimulated $CX^{c/-}$, $CX^{c/-}A^{-/-}$ and control ($X^{c/c}$) splenic B cells with αCD40/IL4 for 4 days to promote IgG1 CSR and assayed metaphases for *IgH* breaks and translocations via fluorescence *in situ* hybridization (FISH) with 5′ and 3′ *IgH* probes. While general chromosomal breaks, as expected, were largely AID-independent in activated $CX^{c/-}$ splenic B cells (Suppl. Table 2), the vast majority of *IgH* breaks were AID-dependent (Fig. 1a and Suppl. Table 1).

RAG-dependent *Igλ* Breaks and Translocations in Xrcc4-deficient Splenic B Cells

We assayed activated $CX^{c/-}$ splenic B cells for *Igλ* breaks via metaphase FISH with 5′ and 3′ *Igλ* probes that flank the 200kb *Igλ* locus on chromosome 16 (Fig. 1b). After αCD40/IL4 stimulation for 4 days, we found *Igλ* breaks in over 1% of $CX^{c/-}$ B cells, with none in controls (Fig. 1b and Suppl. Table 3). Moreover, the *Igλ* breaks were frequently translocated (Fig. 1b; Suppl. Fig. 2). Metaphase FISH with BAC probes flanking *Igκ* revealed that 1% of activated $CX^{c/-}$ B cells also harbor *Igκ* breaks/translocations (Fig. 1c; Suppl. Fig. 2; Suppl. Table 4). In contrast, Xrcc4-deficient embryonic stem (ES) cells lacked *Igκ or Igλ* abnormalities (Suppl. Table 5). To elucidate when *Igλ* and *Igκ* breaks occurred, we assayed $CX^{c/-}$ splenic B cells at days 2, 3, and 4 of activation and observed both to accumulate during stimulation, with *Igκ* breaks kinetically preceding *Igλ* breaks (Suppl. Table 3, 4, and 6; Suppl. Fig. 3). We also assayed for *Igλ* breaks via 3D interphase FISH with 5′*Igλ* and 3′*Igλ* probes (Fig. 1d). *Igλ* breaks were rare in resting (day 0) $CX^{c/-}$ splenic B cells, but occurred in about 1.5% of day 4 activated $CX^{c/-}$ splenic B cells (Fig. 1d; Suppl. Fig 4, Table 7). We conclude that *Igλ* and *Igκ* breaks occur during expansion of activated $CX^{c/-}$ splenic B cells, a conclusion supported by our findings that p53 deficiency did not markedly enhance *Igλ* breaks (Suppl. Table 3) and that 50% of metaphases with *Igλ* breaks retained the acentric chromosome 16 fragment (Fig. 1b, data not shown).

To test AID involvement, we assayed for *Igκ* and *Igλ* breaks in day 4 αCD40/IL4-activated $CX^{c/-}A^{-/-}$ B cells and found a comparable frequency as in $CX^{c/-}$ B cells (Fig. 1b,c, Suppl. Table 3 and 4, Suppl. Fig. 5). Similar to earlier studies[32,39], we found only very low RAG expression in activated normal and $CX^{c/-}$ splenic B cells (data not shown). To further assess RAG involvement, we bred a LoxP-flanked *Rag2* conditional allele ($RAG^{c/c}$)[40] into the $CX^{c/-}$ genotype to generate $CX^{c/-}RAG^{c/c}$ or $CX^{c/-}RAG^{c/-}$ (*"$CX^{c/-}RAG^{c}$"*) mice. Upon activation, the RAG conditional allele was largely deleted in day 3 and 4 activated $CX^{c/-}RAG^{c}$ cells (Suppl. Fig. 6). While *IgH* break frequency was comparable between $CX^{c/-}$ and $CX^{c/-}RAG^{c}$ B cells, *Igλ* break frequency was significantly reduced in $CX^{c/-}RAG^{c}$ B cells (Fig. 1a,b, Suppl. Table 1 and 3). Thus, in activated $CX^{c/-}$ splenic B cells, *IgH* breaks are AID-dependent and RAG-independent; while *Igλ* breaks are AID-independent and mostly RAG-dependent. *Igκ* breaks were not significantly reduced in activated $CX^{c/-}RAG^{c}$ B cells (Fig. 1c, Suppl. Table 4), suggesting they either are not initiated by AID or RAG or their earlier kinetic onset allows accumulation before RAG activity is eliminated.

RAG and AID Collaborate in Generating High Frequency *IgH/Igλ* Translocations

We employed sequential FISH to ask if *IgH*, *Igκ* or *Igλ* breaks occurred simultaneously in $CX^{c/-}$ B cell metaphases. Analyses of over 2000 day 4 αCD40/IL4-activated $CX^{c/-}$ B cell

metaphases revealed none had both *Igκ* and *Igλ* breaks (Suppl. Fig. 7). However, analyses with a Jκ-Cκ probe showed that nearly 50% of metaphases with a broken *Igλ* had deleted Jκ-Cκ on one or both alleles (Suppl. Fig.8), similar to secondary V(D)J recombination events in CXP B lymphomas[36]. We found one *Igκ/IgH* translocation in over 2000 activated $CX^{c/-}$ B cell metaphases, consistent with a high frequency but at levels just below ready cytogenetic measurement (Suppl. Fig. 9a). Nearly 60% of metaphases with *Igλ* breaks also had *IgH* breaks and/or translocations and about 20% of these retained both centric and acentric portions of chromosome 12 and 16 (Suppl. Fig. 7; Suppl Fig. 9b,c; not shown), suggesting attempted V(D)J recombination and CSR in the same or successive cell cycles. In this regard, combined FISH with *Igλ* and *IgH* probes and chromosome paints revealed that 30% of *Igλ* translocations involved *IgH* (e.g. Fig. 2a; Suppl. Fig. 9b,c). As many *IgH/Igλ* translocations resulted in dicentrics with 3′*Igλ* and 3′ *IgH* probes juxtaposed (Suppl. Fig. 9b), we performed FISH with these probes simultaneously, which revealed AID-dependent *IgH/Igλ* translocations in about 0.2% of $CX^{c/-}$ B cells (Fig. 2a, Suppl. Table 8, Fig. 10). We conclude that unrepaired RAG-dependent *Igλ* breaks in activated $CX^{c/-}$ splenic B cells are frequently fused to AID-dependent *IgH* breaks in the same cell to form chromosome 12/16 translocations.

We isolated *IgH/Igλ* translocation junctions from $CX^{c/-}$ B cells via PCR (Suppl. Fig. 10), and found most fused Sμ to sequences downstream of Jλ1/Jλ3 V(D)J recombination signal sequences (Fig.2b, Suppl. Fig.11). Consistent with AID-initiated *IgH* breaks joined to RAG-initiated *Igλ* breaks, point mutations and other alterations were observed in *IgH*- but not *Igλ*-derived junctional sequences (Suppl. Fig.11). Consistent with RAG-initiated breaks resolved in the absence of NHEJ, *Igλ* junctions were at variable distances downstream of Jλ1 and Jλ3. Finally, most *IgH/Igλ* junctions contained microhomologies indicative of A-EJ (Suppl. Fig. 11). We conclude that, in activated splenic $CX^{c/-}$ B cells, A-EJ joins RAG-induced *Igλ* breaks to AID-initiated *IgH* breaks at high frequency.

Cell-type Specific and Focal Co-localization of *IgH* and *Igλ* in B Cell Interphase Nuclei

3D interphase FISH with 3′*IgH* and 3′*Igλ* probes revealed co-localization of the loci (≤0.5μm apart) in about 14% of resting (day 0) and 7-8% of day 3.5 αC40/IL4-activated control and $CX^{c/-}$ splenic B cells (Fig. 3a-d; Suppl. Table 9,10). As there are no *IgH* or *Igλ* breaks in resting B cells (Figs. 1a, d), and AID-initiated breaks begin at day 2[41], we conclude *IgH* and *Igλ* co-localize before and after DSB induction and that Xrcc4 deficiency does not alter this association. To assess cell-type specificity, we assayed wt thymocyte and ES cell interphase nuclei and found only low-level *IgH/Igλ* co-localization (Fig. 3c, Suppl. Table 9). To examine specificity of the *IgH/Igλ* association within chromosome 16, we tested co-localization of *IgH* with two control loci (C2 and K10), which map, respectively, about 15Mb telomeric or centromeric to *Igλ* (Fig. 3b). *IgH/C2* co-localization was at background levels in resting and activated B cells and thymocytes, while *IgH/K10* co-localization occurred at substantially lower levels than *IgH/Igλ* co-localization (Fig. 3c, Suppl. Table 11). Therefore, *IgH* and *Igλ* co-localization is cell-type specific and focal on chromosome 16 with respect to *Igλ*. Notably, *IgH* and *Igκ* also specifically and focally, at least with respect to *Igκ*, co-localize in about 5% of splenic B cells (Suppl. Fig.12, Table 12).

The c-myc DSB Frequency is Rate-limiting for *IgH/c-myc* Translocations

Given that CXP tumors routinely have *IgH/c-myc* translocations[36], we tested for *IgH/c-myc* co-localization in B cell nuclei via 3D interphase FISH (Fig. 4b). Approximately, 4-6% of resting, 15′ activated and 3.5 day activated control or $CX^{c/-}$ B cell nuclei had co-localized

IgH/c-myc signals (Fig. 4b,c; Suppl. Table 13), which were specific as *IgH* and *c-myc* did not co-localize in ES cells (Fig. 4c; Suppl. Table 13). While *c-myc* breaks and *IgH/c-myc* translocations were too infrequent to detect via FISH (Suppl. Table 14), PCR revealed an approximately 5-fold increase in *IgH/c-myc* translocations in activated $CX^{c/-}$ B cells over low ($<1\times10^{-6}$/cell) control levels (Fig. 4a; Suppl. Fig.13 and Table 15). Based on frequent *IgH* breaks and *IgH/c-myc* co-localization, we hypothesized *c-myc* breaks to be rate-limiting for *IgH/c-myc* translocations. To test this, we introduced 25 tandemly arrayed ISceI endonuclease target sites[42] into the *c-myc* first intron to create the $c\text{-}myc^{25IsceI}$ allele (Fig. 4d; Suppl. Fig. 14). The array was used to increase ISceI cut frequency. Then, αCD40/IL4-activated peripheral B cells heterozygous for the $c\text{-}myc^{25IsceI}$ allele ($c\text{-}myc^{25ISceI/wt}$) or wt control B cells ($c\text{-}myc^{wt/wt}$) were infected with ISceI-expressing or control retrovirus[43] and assayed for *c-myc* breaks via metaphase FISH. Strikingly, *c-myc* chromosomal breaks occurred in approximately 10% of $c\text{-}myc^{25ISceI/wt}$ B cells infected with the ISceI virus, but were absent in the various control B cells (Fig. 4e, Suppl. Table 16). PCR quantification demonstrated that *IgH/c-myc* translocations in ISceI virus-infected activated $c\text{-}myc^{25ISceI/wt}$ B cells were increased by at least 100 fold over control levels (Fig. 4a, Suppl. Fig. 15 and Table 16).

Discussion

We show that some activated $CX^{c/-}$ splenic B cells harbor characteristics of postulated "editing and switching" CXP peripheral B cell lymphoma progenitors[36], including *Igκ* deletions, aberrant *Igλ* V(D)J recombination, *Igλ* translocations, and aberrant *IgH* CSR associated with *IgH* translocations to *c-myc* or *Igλ*. Moreover, our studies clearly reveal V(D)J recombination-related events in $CX^{c/-}$ splenic B cells; because they leave telltale RAG-dependent *Igλ* breaks. We note that cultured splenic B cells do not represent GC B cells[44] and CXP tumor progenitors do not appear of GC origin[36]. Therefore, we suggest that V(D)J recombination events in activated $CX^{c/-}$ splenic B cells and putative CXP lymphoma progenitors may represent peripheral "editing" mediated by low RAG expression, for example, as found in transitional B cells[8,45,46]. While potential physiological roles for such a process are unknown, it may be relevant for peripheral B cells subjected to chronic activation, such as those in gut-associated lymphoid tissues where CXP tumors arise[36]. In this context, we find RAG-dependent *Igλ* breaks in $CX^{c/-}$ mesenteric lymph node B cells taken directly from mice (unpublished data).

Our findings of RAG-initiated chromosomal breaks and translocations in Xrcc4-deficient peripheral B cells raises the possibility that translocations in some human peripheral B cell lymphomas, such as follicular lymphomas, might be initiated by V(D)J recombination in the periphery[15,30]. Our findings also demonstrate that AID and RAG can collaborate to generate frequent *IgH/Igλ* translocations in peripheral $CX^{c/-}$ B cells. It is particularly notable that these *IgH/Igλ* translocations offer no obvious cellular selective advantage. Therefore, their appearance as clonal translocations in CXP lymphomas simply may reflect the frequent occurrence of these translocations in tumor progenitors due to mechanistic factors that include the two loci being frequently broken and spatially proximal. In the latter context, our findings demonstrate that the co-localization of two loci on different chromosomes can be quite focal, implicating aspects of particular loci themselves, beyond broader chromosomal territories[47], as important factors in determining spatial proximity and translocation frequency. Finally, analyses of oncogenic translocations in NHEJ-deficient pro-B and B cell lymphomas[36,48] suggested A-EJ may be translocation prone relative to NHEJ[49,50]. The high frequency of specific translocations catalyzed by A-EJ in non-transformed $CX^{c/-}$ B cells supports this notion.

Methods Summary

Generation of mouse strains utilized

CX$^{c/-}$ mice were generated as previously described[10] and crossed into AID-deficient mice[38] to generate *CX*$^{c/-}$*A*$^{-/-}$ or mice carrying floxed RAG2 alleles[40] to generate *CX*$^{c/-}$*RAG*^{c} lines. We inserted a cassette containing 25 tandem ISceI target sites into the 1st intron of *c-myc* by gene targeting (details in online Methods). Mice were analyzed as outlined in the text at 8–16 weeks of age. The Institutional Animal Care and Use Committee of Children's Hospital (Boston, Massachusetts) approved all animal work.

Splenic B cell Purification, Activation in Culture, Retroviral Infection and CSR Assays

CD43^{-} B cells were isolated from spleen, cultured, and assayed for CSR as previously described[10,22]. Cells were sampled on various days for DNA isolation, flow cytometry analyses and metaphase preparation. Retroviral infection was performed as previously described[43] (details in online Methods).

Two-color FISH and telomere-FISH

Metaphase spreads from αCD40/IL4-activated B cell cultures were prepared and two-color FISH to detect *IgH*, *Igκ*, *Igλ* or *c-myc* chromosomal aberrations and telomere staining (T-FISH) to detect general aberrations were performed as previously described[10]. FISH probes are detailed in online Methods.

3D interphase FISH

3D FISH was performed as described previously[32] (details in online Methods). Images of approximately 50 serial optical sections spaced by 0.2 microns were captured with Marianas spinning disk confocal microscope (63×) with a CCD detector (Intelligent Imaging Innovations) and analyzed with Slidebook software (Intelligent Imaging Innovations).

PCR assay to detect *IgH/c-myc* or *IgH/Igλ* translocations

IgH/c-myc translocation junctions were amplified by PCR from genomic DNA prepared from αCD40/IL4 activated splenic B cells using primers previously described[26]. PCR products were run on agarose gels and hybridized with an internal *c-myc* oligo. *IgH/Igλ* translocations were amplified using nested primers for *Sμ* and *Jλ*. PCR products were hybridized with *Jλ* and *IgH* probes, the bands positive for both probes were cloned into the pGEM-T vector (Promega), sequenced and analyzed using Lasergene software and the NCBI database. Primer sequences and PCR conditions are detailed in online Methods.

Supplementary Material

Refer to Web version on PubMed Central for supplementary material.

Acknowledgments

We thank Alt lab members for discussions, and Y.L. Chen, J. M. Bianco and M. Moghimi for technical assistance. This work was supported by NIH grant 5P01CA92625 and a Leukemia and Lymphoma Society of America (LLS) SCORE grant (to F.W.A. and K.R.). M.G. is and J.H.W. was a Special Fellow of LLS. J.H.W. and D.R.W. are supported by an NIH training grant and C.T.Y. was supported by an NCI training grant. A.N. is supported by the Intramural Research program of the NIH, NCI, Center for Cancer Research. F.W.A. is an Investigator of the Howard Hughes Medical Institute.

References

1. Jung D, Alt FW. Unraveling V(D)J recombination; insights into gene regulation. Cell 2004;116:299–311. [PubMed: 14744439]
2. Rooney S, Chaudhuri J, Alt FW. The role of the non-homologous end-joining pathway in lymphocyte development. Immunol Rev 2004;200:115–31. [PubMed: 15242400]
3. Bassing CH, Swat W, Alt FW. The mechanism and regulation of chromosomal V(D)J recombination. Cell 2002;109(Suppl):S45–55. [PubMed: 11983152]
4. Gorman JR, Alt FW. Regulation of immunoglobulin light chain isotype expression. Adv Immunol 1998;69:113–81. [PubMed: 9646844]
5. Gay D, Saunders T, Camper S, Weigert M. Receptor editing: an approach by autoreactive B cells to escape tolerance. J Exp Med 1993;177:999–1008. [PubMed: 8459227]
6. Tiegs SL, Russell DM, Nemazee D. Receptor editing in self-reactive bone marrow B cells. J Exp Med 1993;177:1009–20. [PubMed: 8459201]
7. Nemazee D. Receptor editing in lymphocyte development and central tolerance. Nat Rev Immunol 2006;6:728–40. [PubMed: 16998507]
8. Jankovic M, Casellas R, Yannoutsos N, Wardemann H, Nussenzweig MC. RAGs and regulation of autoantibodies. Annu Rev Immunol 2004;22:485–501. [PubMed: 15032586]
9. Chaudhuri J, et al. Evolution of the immunoglobulin heavy chain class switch recombination mechanism. Adv Immunol 2007;94:157–214. [PubMed: 17560275]
10. Yan CT, et al. IgH class switching and translocations use a robust non-classical end-joining pathway. Nature 2007;449:478–82. [PubMed: 17713479]
11. Nemazee D, Weigert M. Revising B cell receptors. J Exp Med 2000;191:1813–7. [PubMed: 10839798]
12. Seagal J, Melamed D. Role of receptor revision in forming a B cell repertoire. Clin Immunol 2002;105:1–8. [PubMed: 12483988]
13. Wilson PC, et al. Receptor revision of immunoglobulin heavy chain variable region genes in normal human B lymphocytes. J Exp Med 2000;191:1881–94. [PubMed: 10839804]
14. Goossens T, Brauninger A, Klein U, Kuppers R, Rajewsky K. Receptor revision plays no major role in shaping the receptor repertoire of human memory B cells after the onset of somatic hypermutation. Eur J Immunol 2001;31:3638–48. [PubMed: 11745384]
15. Kuppers R, Dalla-Favera R. Mechanisms of chromosomal translocations in B cell lymphomas. Oncogene 2001;20:5580–94. [PubMed: 11607811]
16. Janz S. Myc translocations in B cell and plasma cell neoplasms. DNA Repair (Amst) 2006;5:1213–24. [PubMed: 16815105]
17. Gostissa M, Ranganath S, Bianco JM, Alt FW. Chromosomal location targets different MYC family gene members for oncogenic translocations. Proc Natl Acad Sci U S A 2009;106:2265–70. [PubMed: 19174520]
18. Kozubek S, et al. Distribution of ABL and BCR genes in cell nuclei of normal and irradiated lymphocytes. Blood 1997;89:4537–45. [PubMed: 9192778]
19. Neves H, Ramos C, da Silva MG, Parreira A, Parreira L. The nuclear topography of ABL, BCR, PML, and RARalpha genes: evidence for gene proximity in specific phases of the cell cycle and stages of hematopoietic differentiation. Blood 1999;93:1197–207. [PubMed: 9949162]
20. Nikiforova MN, et al. Proximity of chromosomal loci that participate in radiation-induced rearrangements in human cells. Science 2000;290:138–41. [PubMed: 11021799]
21. Roix JJ, McQueen PG, Munson PJ, Parada LA, Misteli T. Spatial proximity of translocation-prone gene loci in human lymphomas. Nat Genet 2003;34:287–91. [PubMed: 12808455]
22. Osborne CS, et al. Myc dynamically and preferentially relocates to a transcription factory occupied by Igh. PLoS Biol 2007;5:e192. [PubMed: 17622196]
23. Meaburn KJ, Misteli T, Soutoglou E. Spatial genome organization in the formation of chromosomal translocations. Semin Cancer Biol 2007;17:80–90. [PubMed: 17137790]
24. Tsai AG, et al. Human chromosomal translocations at CpG sites and a theoretical basis for their lineage and stage specificity. Cell 2008;135:1130–42. [PubMed: 19070581]

25. Mahowald GK, Baron JM, Sleckman BP. Collateral damage from antigen receptor gene diversification. Cell 2008;135:1009–12. [PubMed: 19070571]
26. Ramiro AR, et al. AID is required for c-myc/IgH chromosome translocations in vivo. Cell 2004;118:431–8. [PubMed: 15315756]
27. Ramiro A, et al. The role of activation-induced deaminase in antibody diversification and chromosome translocations. Adv Immunol 2007;94:75–107. [PubMed: 17560272]
28. Kovalchuk AL, et al. AID-deficient Bcl-xL transgenic mice develop delayed atypical plasma cell tumors with unusual Ig/Myc chromosomal rearrangements. J Exp Med 2007;204:2989–3001. [PubMed: 17998390]
29. Robbiani DF, et al. AID is required for the chromosomal breaks in c-myc that lead to c-myc/IgH translocations. Cell 2008;135:1028–38. [PubMed: 19070574]
30. Jager U, et al. Follicular lymphomas' BCL-2/IgH junctions contain templated nucleotide insertions: novel insights into the mechanism of t(14;18) translocation. Blood 2000;95:3520–9. [PubMed: 10828038]
31. Lieber MR, Yu K, Raghavan SC. Roles of nonhomologous DNA end joining, V(D)J recombination, and class switch recombination in chromosomal translocations. DNA Repair (Amst) 2006;5:1234–45. [PubMed: 16793349]
32. Callen E, et al. ATM prevents the persistence and propagation of chromosome breaks in lymphocytes. Cell 2007;130:63–75. [PubMed: 17599403]
33. Li Z, et al. The XRCC4 gene encodes a novel protein involved in DNA double-strand break repair and V(D)J recombination. Cell 1995;83:1079–89. [PubMed: 8548796]
34. Gao Y, et al. A critical role for DNA end-joining proteins in both lymphogenesis and neurogenesis. Cell 1998;95:891–902. [PubMed: 9875844]
35. Soulas-Sprauel P, et al. Role for DNA repair factor XRCC4 in immunoglobulin class switch recombination. J Exp Med 2007;204:1717–27. [PubMed: 17606631]
36. Wang JH, et al. Oncogenic transformation in the absence of Xrcc4 targets peripheral B cells that have undergone editing and switching. J Exp Med 2008;205:3079–90. [PubMed: 19064702]
37. Kraus M, Alimzhanov MB, Rajewsky N, Rajewsky K. Survival of resting mature B lymphocytes depends on BCR signaling via the Igalpha/beta heterodimer. Cell 2004;117:787–800. [PubMed: 15186779]
38. Muramatsu M, et al. Class switch recombination and hypermutation require activation-induced cytidine deaminase (AID), a potential RNA editing enzyme. Cell 2000;102:553–63. [PubMed: 11007474]
39. Gartner F, Alt FW, Monroe RJ, Seidl KJ. Antigen-independent appearance of recombination activating gene (RAG)-positive bone marrow B cells in the spleens of immunized mice. J Exp Med 2000;192:1745–54. [PubMed: 11120771]
40. Hao Z, Rajewsky K. Homeostasis of peripheral B cells in the absence of B cell influx from the bone marrow. J Exp Med 2001;194:1151–64. [PubMed: 11602643]
41. Schrader CE, Linehan EK, Mochegova SN, Woodland RT, Stavnezer J. Inducible DNA breaks in Ig S regions are dependent on AID and UNG. J Exp Med 2005;202:561–8. [PubMed: 16103411]
42. Plessis A, Perrin A, Haber JE, Dujon B. Site-specific recombination determined by I-SceI, a mitochondrial group I intron-encoded endonuclease expressed in the yeast nucleus. Genetics 1992;130:451–60. [PubMed: 1551570]
43. Zarrin AA, et al. Antibody class switching mediated by yeast endonuclease-generated DNA breaks. Science 2007;315:377–81. [PubMed: 17170253]
44. Lahvis GP, Cerny J. Induction of germinal center B cell markers in vitro by activated CD4+ T lymphocytes: the role of CD40 ligand, soluble factors, and B cell antigen receptor cross-linking. J Immunol 1997;159:1783–93. [PubMed: 9257841]
45. Monroe RJ, et al. RAG2:GFP knockin mice reveal novel aspects of RAG2 expression in primary and peripheral lymphoid tissues. Immunity 1999;11:201–12. [PubMed: 10485655]
46. Yu W, et al. Continued RAG expression in late stages of B cell development and no apparent re-induction after immunization. Nature 1999;400:682–7. [PubMed: 10458165]

47. Cremer T, Cremer C. Chromosome territories, nuclear architecture and gene regulation in mammalian cells. Nat Rev Genet 2001;2:292–301. [PubMed: 11283701]

48. Zhu C, et al. Unrepaired DNA breaks in p53-deficient cells lead to oncogenic gene amplification subsequent to translocations. Cell 2002;109:811–21. [PubMed: 12110179]

49. Roth DB. Amplifying mechanisms of lymphomagenesis. Mol Cell 2002;10:1–2. [PubMed: 12150897]

50. McVey M, Lee SE. MMEJ repair of double-strand breaks (director's cut): deleted sequences and alternative endings. Trends Genet 2008;24:529–38. [PubMed: 18809224]

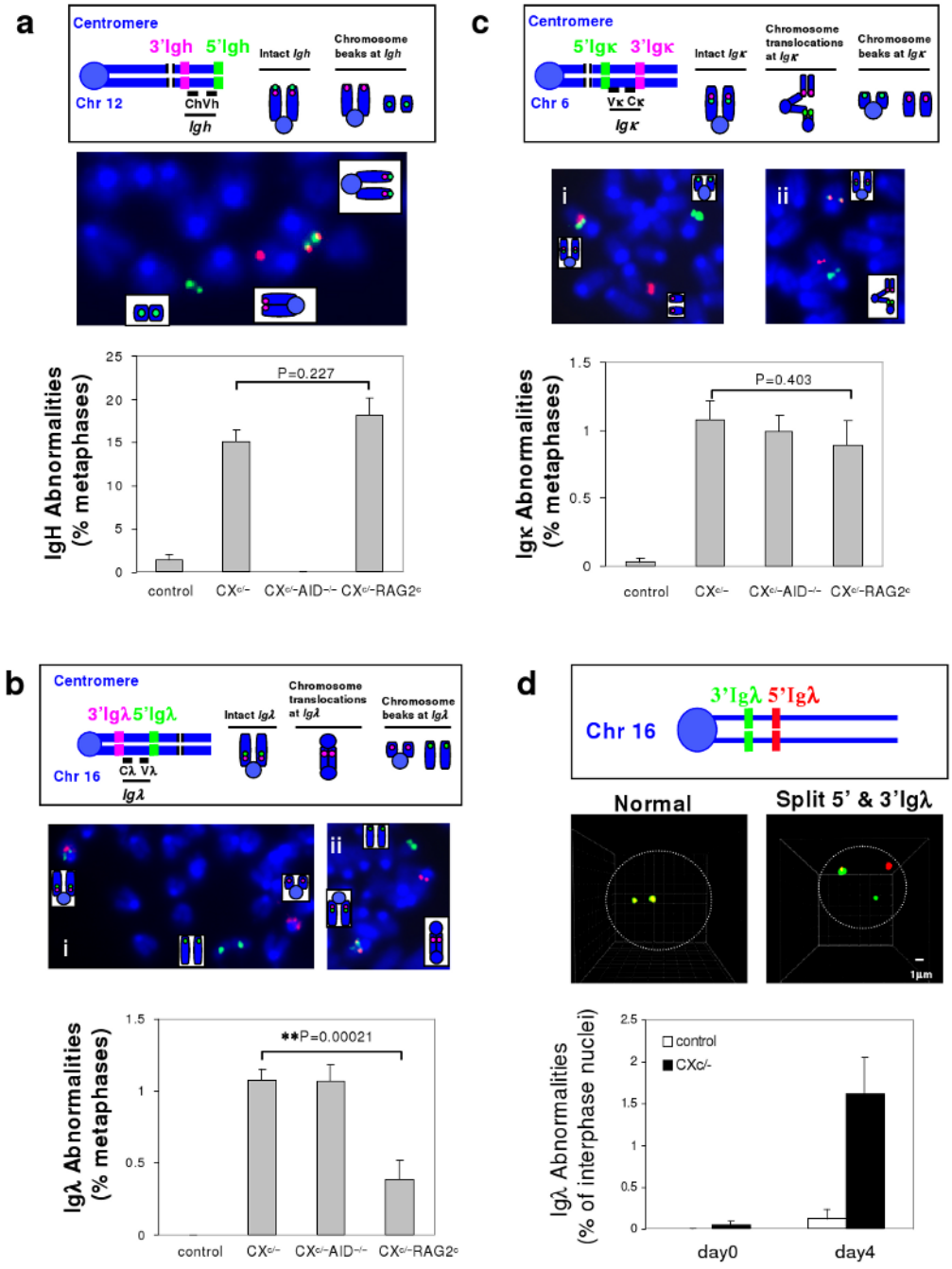

Figure 1. Role of AID and RAG in Generating *IgH*, *Igκ*, and *Igλ* breaks in CX$^{c/-}$ Splenic B cells

a, Upper: Diagram of *IgH* FISH probes. An intact *IgH* shows co-localized red and green signals while a broken locus appears as split red and green signals. **Middle:** Example of metaphase FISH showing *IgH* breaks. **Lower:** Quantification of *IgH* abnormalities in day4 αCD40/IL4-activated control (n=6), *CX$^{c/-}$* (n=9), *CX$^{c/-}$A$^{-/-}$* (n=5) and *CX$^{c/-}$RAG^{c}* (n=8) splenic B cells (details in Suppl. Table 1). **b, Upper:** Diagram of *Igλ* FISH probes. Intact *Igλ* shows co-localized green and red signals, *Igλ* breaks appear as split green and red signals, either free or in translocations. **Middle:** Examples of metaphase FISH showing *Igλ* breaks (left) and an *Igλ* break and dicentric translocation (right). **Lower:** Quantification of *Igλ* abnormalities in day4 αCD40/IL4-activated control (n=11), *CX$^{c/-}$* (n=11), *CX$^{c/-}$A$^{-/-}$* (n=3),

$CX^{c/-}RAG2^{c}$ (n=8) splenic B cells (details in Suppl. Table 3). **c, Upper:** Diagram of *Igκ FISH* probes. *Igκ* breaks are scored similarly as *Igλ* breaks. **Middle:** Examples of metaphase FISH showing an *Igκ* break (left) and *Igκ* break and translocations (right), involving both centromeric and telomeric portions of chromosome 6. **Lower:** Quantification of *Igκ* abnormalities in day4 αCD40/IL4-activated control (n=10), *$CX^{c/-}$* (*n*=11), *$CX^{c/-}A^{-/-}$* (n=3), *$CX^{c/-}RAG^{c}$* (n=7) splenic B cells (details in Suppl. Table 4). **d, Upper:** Diagram of *Igλ* 3D interphase FISH Probes. **Middle:** Representative 3D interphase FISH showing intact *Igλ* (co-localization of green and red signals) and *Igλ* breaks (split green and red signals) (details in Suppl. Fig. 4). **Lower:** Quantification of *Igλ* abnormalities by 3D interphase FISH on day 0 (n=3) or day 4 (n=3) αCD40/IL4-activated splenic B cells. We could not do similar assays for *Igκ* due to the large size of this locus (greater than 3Mb). In all panels, data are presented as mean ± s.e.m. Statistical analyses were calculated by a Student's t-Test with two-tailed distribution.

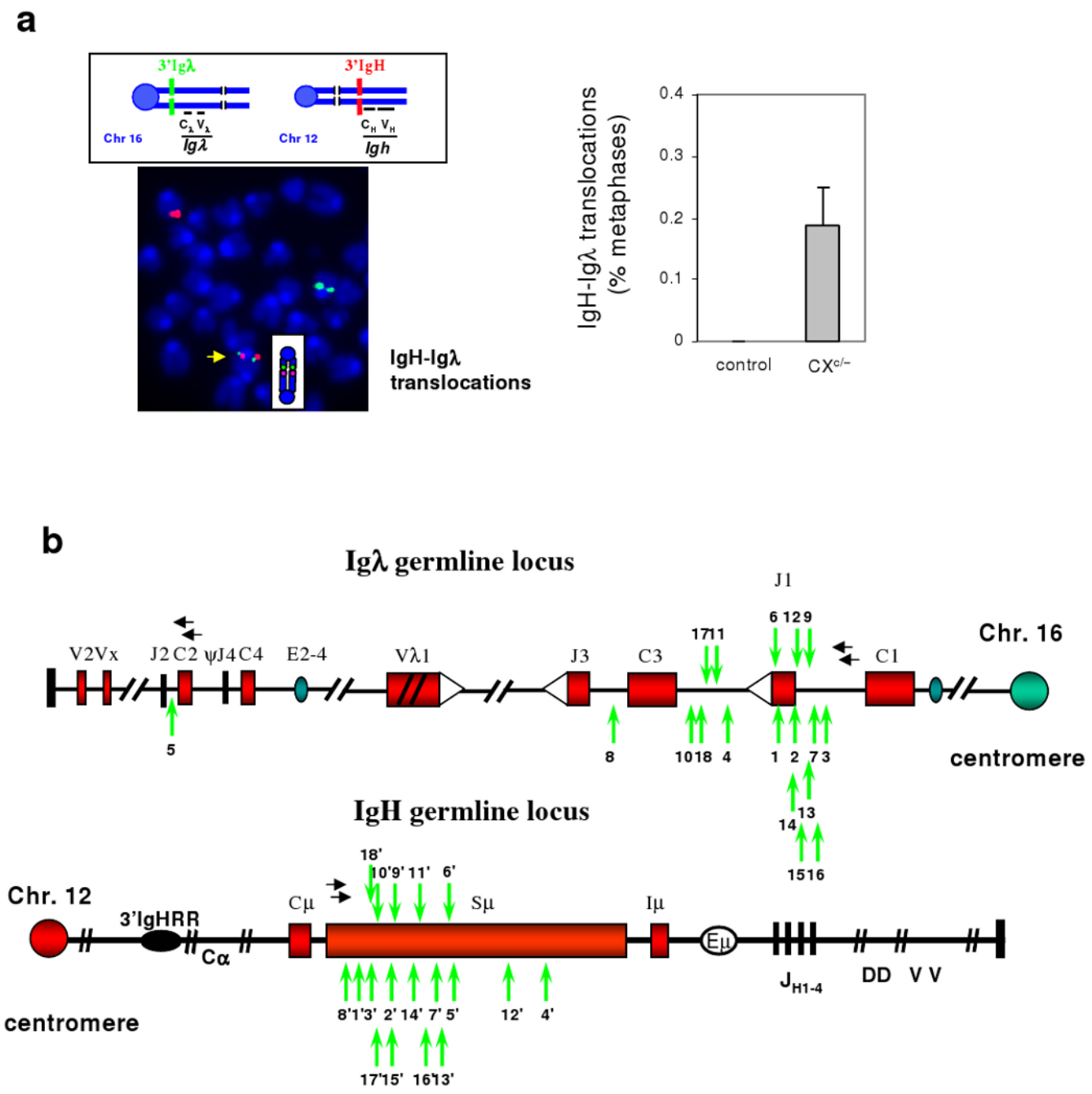

Figure 2. Frequent *IgH/Igλ* translocations in activated Xrcc4-deficient splenic B cells

a, Top left: Diagram showing *3′Igλ* probe (green) on chromosome 16 and *3′IgH* probe (red) on chromosome 12. **Bottom left:** Representative *Igλ/IgH* translocation showing green and red signals juxtaposed on a dicentric chromosome (yellow arrow). **Right**: Quantification of *IgH/Igλ* translocations in day4 αCD40/IL4-activated control (n=2) or $CX^{c/-}$ (n=4) B cells analyzed by metaphase FISH (details in Suppl. Table 8). Data are presented as mean ± std. **b,** PCR-isolated *Igh/Igλ* translocation junctions from day4 activated $CX^{c/-}$ B cells (n=3) (primers indicated by horizontal black arrows). Junctional sequences are shown in Suppl. Fig. 11. A vertical green arrow indicates breakpoints. For a given translocation, the same

number is used to indicate the corresponding *IgH* and *Igλ* breakpoints, with the *IgH* breakpoint denoted by a (') symbol.

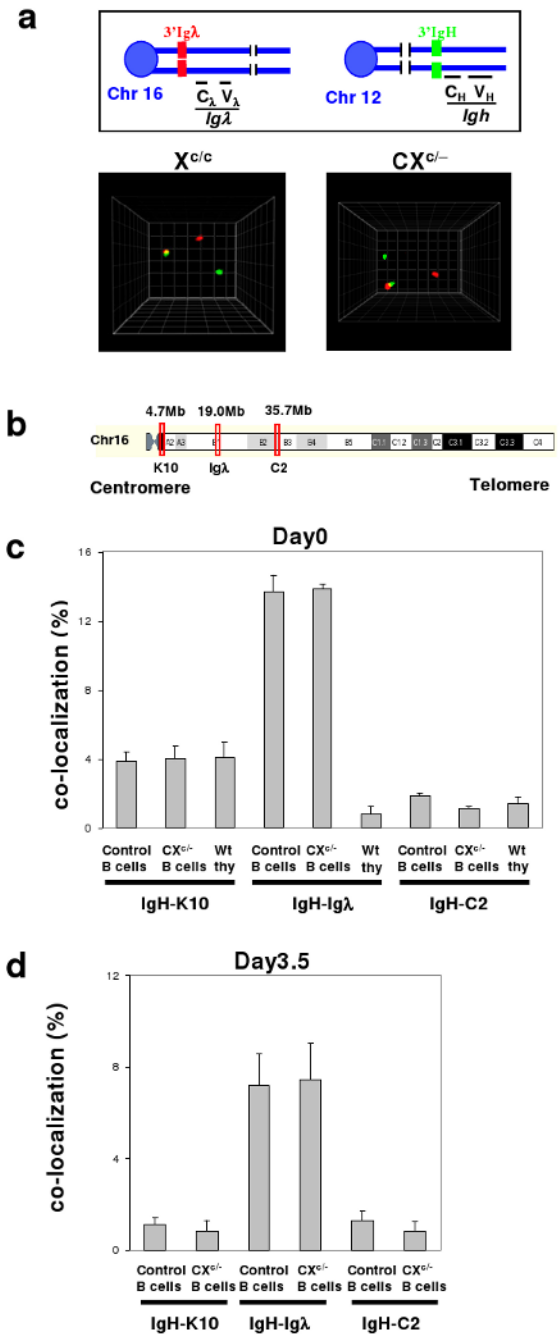

Figure 3. Frequent cell-type and Igλ locus-specific *IgH/Igλ* co-localization

a, Top: Diagram showing 3′*IgH* (green) and 3′*Igλ* (red) probes used for 3D interphase FISH. **Bottom:** Representative co-localization of *IgH/Igλ* in day 0 control and $CX^{c/-}$ B cell interphase nuclei. **b,** Schematic map of *Igλ*, *C2* and *K10* BAC probes on chromosome 16. **c,** Quantification of co-localization of *IgH-Igλ*, *IgH-C2*, or *IgH-K10* loci in nuclei of day 0 control and $CX^{c/-}$ splenic B cells and in nuclei of thymocytes (details in Suppl. Tables 9 and 11). **d,** Quantification of co-localization of *IgH-Igλ*, *IgH-C2*, or *IgH-K10* loci in day3.5-activated control or $CX^{c/-}$ peripheral B cells (details in Suppl. Table 10). At least three mice were analyzed per data set; data are presented as mean ± s.e.m.

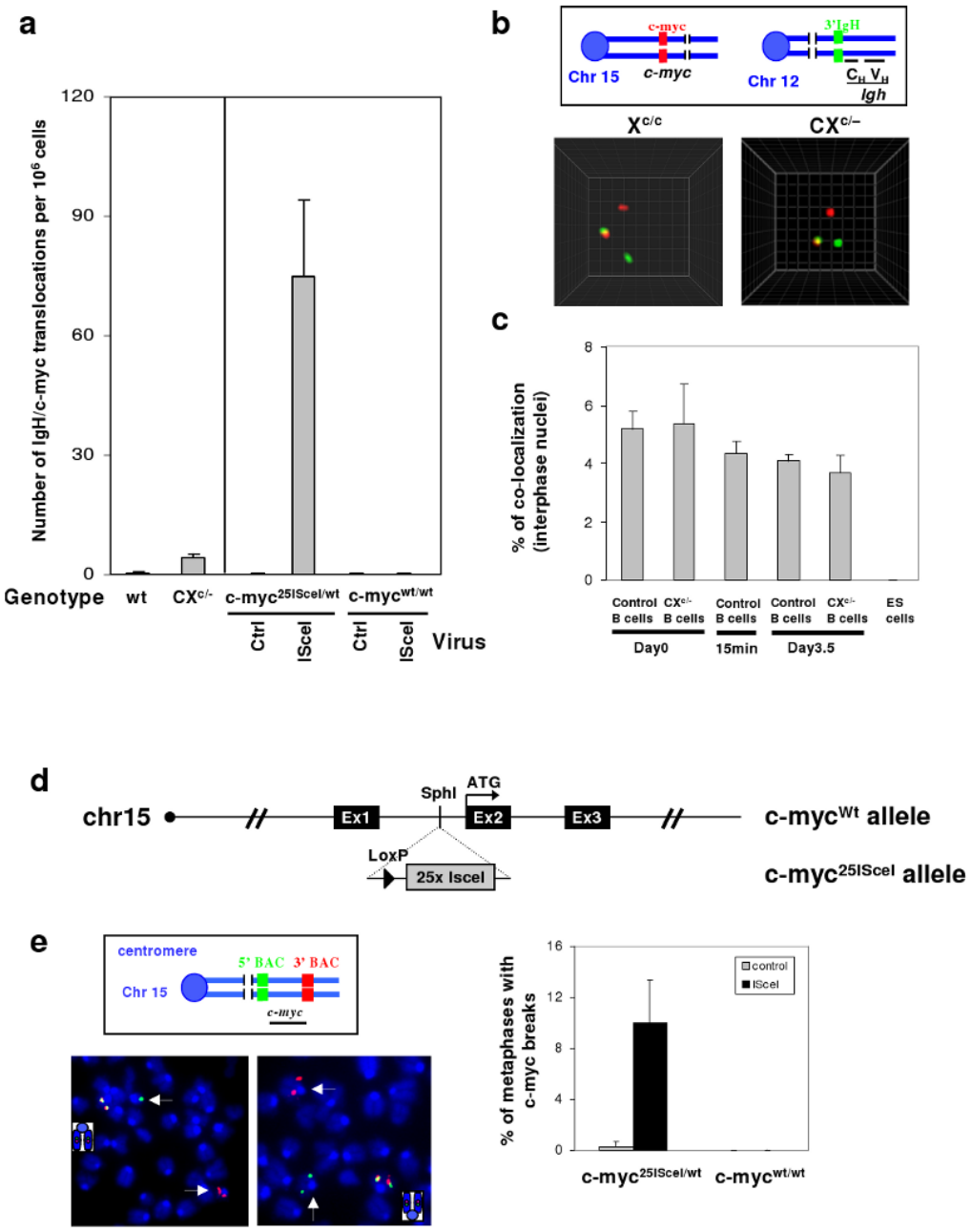

Figure 4. DSBs in *c-myc* are rate-limiting for *IgH/c-myc* translocations in activated splenic B cells

a, Frequency of *IgH/c-myc* translocations from day4 αCD40/IL4-activated wt (n=4) and $CX^{c/-}$ (n=4) splenic B cells, or B cells harboring $c\text{-}myc^{25ISceI/wt}$ (n=3) or $c\text{-}myc^{wt/wt}$ (n=1) infected with either control or ISceI-expressing retrovirus (details in Suppl. Fig. 13 and 15). **b, Top:** Schematic showing *c-myc* (red) probe on chromosome 15 and *3'IgH* (green) probe on chromosome 12. **Bottom:** Representative images of *IgH/c-myc* co-localization in day 0 control and $CX^{c/-}$ B cell interphase nuclei. **c,** Quantification of *IgH/c-myc* association by 3D interphase FISH in control and $CX^{c/-}$ splenic B cells (n=3), and ES cells (n=3). Cells were analyzed at the indicated time points before or after stimulation. **d,** Schematic showing the wt *c-myc* allele ($c\text{-}myc^{wt}$) and the modified *c-myc* allele containing 25 ISceI sites ($c\text{-}myc^{25ISceI}$). **e, Top left:** Diagram of *c-myc* FISH probes. **Bottom left:** Representative *c-myc*

abnormalities in αCD40/IL-4-activated *c-myc*$^{25ISceI/wt}$ B cells infected with IsceI-expressing retrovirus, appearing as green and red signals on separate chromosome fragments (white arrows). **Bottom right:** Quantification of *c-myc* breaks by metaphase FISH on day4 αCD40/IL4-activated B cells harboring either *c-myc*$^{25ISceI/wt}$ (n=4) or *c-myc*$^{wt/wt}$ (n=1) alleles after infection with control or ISceI-expressing retrovirus. Data are presented as mean ± std (details in Suppl. Table 16). High titer retrovirus infection appears to inhibit end joining allowing break visualization (see online methods).